



ELSEVIER

Journal of Chromatography A, 675 (1994) 29–45

JOURNAL OF  
CHROMATOGRAPHY A

# Synthesis and characterization of silica-based aliphatic ion exchangers

Laura A. Ciolino, John G. Dorsey\*

*Department of Chemistry, University of Cincinnati, Cincinnati, OH 45221-0172, USA*

(Received January 25th, 1994)

## Abstract

The chemical literature describing preparation of aliphatic ion exchangers is limited, and although such phases are available commercially, the synthetic schemes are proprietary. The course of our research required the preparation of silica-based aliphatic cation and anion exchangers for which the desired base silica and/or ligand properties were not commercially available. We developed synthetic schemes to prepare silica-based aliphatic sulfonic acid, carboxylic acid and quaternary ammonium ion-exchange phases with active exchange capacities of 0.2–0.9  $\mu\text{mol}/\text{m}^2$ . Multiple techniques were used to characterize the intermediate and final phases produced in the syntheses, including Fourier transform diffuse reflectance infrared spectroscopy, spot tests, elemental analysis, acid–base titration and elution analysis.

## 1. Introduction

We recently investigated the feasibility of using chromatographic silica-based stationary phases as substrates for room temperature phosphorescence. The course of our research required the preparation of aliphatic cation and anion exchangers for which the desired base silica and/or ligand properties were not commercially available. Our interest was in both strong and weak aliphatic ion exchangers, specifically sulfonic acids, carboxylic acids, quaternary amines and amines.

A survey of the literature showed that the vast majority of ion exchangers contain aromatic moieties, and the corresponding synthetic schemes rely on the reactivity of the aromatic

moiety for success. Aromatic moieties could not be tolerated for our application due to their high phosphorescence background. Of the limited literature describing aliphatic ion exchangers, there are several which describe preparation of alkylsulfonic acids or sulfonates. However, except for the aminoalkyl phases, the aliphatic ion exchangers of interest cannot be directly prepared via a one-step coupling reaction to silica because of cross-reactions which would occur with such functional silanes. Therefore, derivatization schemes to prepare these phases involve the coupling of a precursor silane with silica in the first step, followed by conversion of the precursor functional group to the desired functional group in one or more subsequent reactions. Cleavage of the original silane in the subsequent reaction step(s), and low conversion represent the major problems.

\* Corresponding author.

We investigated synthetic schemes to prepare aliphatic sulfonic acid, carboxylic acid and quaternary ammonium phases. In all cases, we were able to prepare the desired phases with *active* exchange capacities between 0.2 and 0.9  $\mu\text{mol}/\text{m}^2$ . Details of the synthetic schemes developed and suggestions for further optimization of the schemes investigated are presented.

Another challenging aspect of synthetic research for derivatized silicas is the characterization of the intermediate and final phases. Characterization comprises both qualitative and quantitative analysis of the attached ligands, including confirmation that the target functional groups are present intact on the surface. The difficulty arises because the “analyte” (attached ligands) represents only a small percentage of the “sample” (derivatized silica), and the sample is an insoluble solid. A combination of techniques must be used in order to provide even an adequate characterization.

Infrared (IR) spectroscopy is the most frequently used tool for functional group analysis of derivatized silicas [1–6], although solid-state NMR has also been used [7–9]. With the availability of Fourier transform diffuse reflectance IR spectroscopy (FT-DRIFT) [10], the IR spectra of solid samples are relatively easy to obtain, but the analysis is still complicated by the large background absorbance of silica. IR bands for the attached ligands can be observed directly only in the limited spectral regions which are free of the background. Signal averaging and background subtraction are frequently used to improve the quality and appearance of the spectra. Sample preparation usually involves dilution of the solid phase in a non-absorbing matrix such as KCl. Murthy and Leyden [11] showed that FT-DRIFT could also be used for quantitative determination of ligand coverage under dilute conditions (<17% silica phase in KCl matrix) where the Kubelka–Munk function is linear with respect to concentration. In that work, the absorbance for the aminopropyl ligand (CH stretch) was referenced to the silica Si–O combination band at  $1870\text{ cm}^{-1}$ . Correlation of the IR response with a second independent method was required for absolute quantitation.

Solid-state NMR has emerged as a powerful tool for the study of derivatized silicas beyond the simple identification of attached ligand functional groups. Solid-state NMR has been used to discriminate modes of attachment for mono-, di- and trifunctional silanes [7], to observe residual adsorbed solvents such as methanol [7,12], and to study the mobility of bonded alkyl chains as a function of chain length and position along the chain [13,14]. This detailed phase characterization comes at the expense of extensive sample preparation (drying under vacuum for hours or days) and sampling time.

Elemental analysis and determination of ion-exchange capacity are the most frequently used tools for quantitative analysis. While elemental analysis is especially useful for one-step coupling reactions, it is virtually impossible to track the course of a multi-step synthetic sequence with such limited information. Another technique which has been used for quantitative analysis is cleavage of the attached silane via acidic or basic hydrolysis followed by GC–MS [15–17] or GC–FID [18–20], but this technique is restricted to silanes which form volatile dimers upon coupling.

In the present study, FT-DRIFT was used in conjunction with wet chemical techniques (spot tests) for the functional group analysis of alkyl-, ester-, thiol- and amine-containing phases. The shape of the acid–base titration curves were used to characterize the cation-exchange phases as strong (sulfonic) or weak (carboxylic) acids. Elemental analysis and exchange capacity determinations (titration or elution) were used for quantitative analysis. The results are presented along with a perspective of the capabilities and limitations of each of the applied techniques.

## 2. Experimental

The base silicas used and their properties are summarized in Table 1. Prior to derivatization, all silicas were acid washed, and then dried overnight at  $150^\circ\text{C}$  under vacuum. Acid washing comprised refluxing in 0.1 M  $\text{HNO}_3$  overnight followed by water washes to neutrality. All

Table 1  
Summary of base silica properties

Silica	Particle diameter ( $\mu\text{m}$ )	Pore diameter ( $\text{\AA}$ )	Shape	Specific surface area ( $\text{m}^2/\text{g}$ )
Waters Nova	5	100	Spherical	119
Davisil	20–30	–	Irregular	300
Waters Nova	12	60	Spherical	114
Supelco	5	100	Spherical	175
Waters Resolve	5	90	Spherical	175
Jones Apex PM 300	5	100	Spherical	170

Silicas in order discussed in text. All information based on manufacturers' literature or contact.

silanes were used as received from Huls America. All solvents were Fisher certified-ACS grade, except for methanol which was Fisher HPLC grade. Reaction solvents were distilled just before use as follows: dichloromethane over  $\text{P}_2\text{O}_5$  under dry nitrogen; dimethylformamide (DMF) over BaO under vacuum; dimethyl sulfoxide (DMSO) over CaH under vacuum; methyl ethyl ketone and toluene over  $\text{CaCl}_2$  under dry nitrogen. All wash solvents were used as received. Distilled water was filtered through a Barnsted system prior to use. Reagents for all primary coupling reactions, and where noted for secondary reactions, were weighed out in a dry box. All primary coupling reactions were conducted under a dry nitrogen purge.

Diethyl disulfide and octanoic acid were used as received from Sigma. Concentrated hydrochloric and sulfuric acids, and 30% aqueous hydrogen peroxide were used as received from Fisher. A solution of 25% trimethylamine (TMA) in methanol was used as received from Kodak. Dimethylaminopyridine (Nepera) was dried overnight at  $80^\circ\text{C}$  and stored in a desiccator prior to use. Sodium iodide (Fisher certified) was recrystallized twice from acetone–diethyl ether, dried *in vacuo* for 2 h at  $50^\circ\text{C}$ , then desiccated. Lithium bromide (MCB reagent grade) was dried for two days at  $105^\circ\text{C}$  *in vacuo* and desiccated prior to use. Lithium iodide (Sigma anhydrous, 99%) was opened in a dry box and used as received.

Silane and other reagent molar excesses were calculated assuming  $5 \mu\text{mol}/\text{m}^2$  reactive silanols for the silica surface. All silanes were added at a  $4 \times$  molar excess. Dimethylaminopyridine (DMAP) catalyst, when used, was added at a  $6 \times$  molar excess.

All elemental analyses were performed by Robertson Microlit Labs. Bonding densities ( $\mu\text{mol}/\text{m}^2$ ) were calculated from elemental analyses according to Eq. 1. Eq. 1 is a modification of Berendsen and De Galan's original equation [6] which has been generalized for any element. A blank carbon level of 0.1% was obtained for the Waters 12- $\mu\text{m}$  underivatized silica. This corresponds to a blank "bonding density" of  $0.15 \mu\text{mol}/\text{m}^2$  for a propyldimethylsilane. The percentage of silane cleavage occurring in secondary or tertiary reactions was calculated from the difference in percent of a given element before *vs.* after the reaction.

$$\alpha (\mu\text{mol}/\text{m}^2) = \frac{\%E \cdot 10^6}{n_E M_{a,E} S \cdot \left[ 100 - \left( \frac{\%E}{M_{a,E} n_E} \right) M_{r,L} \right]} \quad (1)$$

where  $\alpha$  = bonding density,  $\%E$  = mass% element,  $n_E$  = number of atoms of element in ligand fragment,  $M_{a,E}$  = atomic mass of element,  $S$  = specific surface area of silica ( $\text{m}^2/\text{g}$ ) and  $M_{r,L}$  = molecular mass of ligand fragment attached.

Exchange capacities for cation-exchange

phases were determined by manual titration with 0.01 M NaOH, pH electrode detection. A complete titration curve was recorded for each phase. Exchange capacities were calculated from the volume of NaOH required to neutralize the silica dispersion to a pH of 7 for sulfonic acid phases and a pH of 8 for carboxylic acid phases. The solvent was 20% aqueous methanol. Exchange capacities for quaternary ammonium anion-exchange phases were determined by nitrate elution as described by Warth *et al.* [21]. The phases were converted to the nitrate form by washing with 0.5 M NaNO<sub>3</sub> at a pH of 4, and then washed with water to remove the excess nitrate. The bound nitrate was then eluted with 0.05 M Na<sub>2</sub>SO<sub>4</sub> at a pH of 4, and analyzed by UV spectroscopy using the absorbance at 220 nm. Exchange capacities are reported in units of  $\mu\text{mol}/\text{m}^2$  to allow comparison among ion-exchange phases with base silicas of differing specific surface area. Units of  $\mu\text{equiv.}/\text{g}$  are also reported for consideration of the functional properties of the phases.

DRIFT spectra of the silica and derivatized silica phases were taken using a Bio-Rad FTS 60A FT-IR spectrometer with KBr as reference material. The spectra were taken of the neat phases (no dilution in the KBr reference material) without any special sample preparation, other than to keep the phases dry in a desiccator. Resolution was  $8\text{ cm}^{-1}$ , scan speed was 5 kHz, and the aperture was  $1\text{ cm}^{-1}$ . An average of 64 scans was taken for each phase. No background subtraction or smoothing was used. The reflectance data were converted to Kubelka–Munk units using the standard Bio-Rad system software. The bands associated with the attached ligands could be observed on top of the silica background in several spectral regions. Because the solid phases were not diluted in KBr, the reflectance values are outside the linear range of the Kubelka–Munk vs. concentration relation. Therefore, the IR spectra taken are not considered in a strict quantitative sense. However, our experience shows that the appropriate IR absorbances do increase with increasing bonding density for a variety of bonded phases (alkyl, ester, cyclohexenyl), and also increase as the

alkyl chain length increases for reversed phases. Thus, we are satisfied with the semi-quantitative results for the current studies, given that virtually no sample preparation was required.

### 3. Results and discussion

#### 3.1. Sulfonic acid phases

Several researchers have investigated the preparation of sulfonic acid-derivatized silicas via the attachment of an alkyl thiol ligand and its subsequent oxidation. Weigand *et al.* [22] obtained a maximum exchange capacity of  $103\ \mu\text{equiv.}/\text{g}$  ( $0.69\ \mu\text{mol}/\text{m}^2$ ) using hydrogen peroxide as the oxidizing agent for butyl thiol-derivatized silica. Silane cleavage was 50%. Wheals [23] attached a propyl thiol silane at  $1.6\ \mu\text{mol}/\text{m}^2$  and subsequently oxidized the thiol to the sulfonic acid using potassium permanganate in 1 M sulfuric acid. The final phase had a reported exchange capacity of 0.5–0.6 mequiv./g ( $1.4\ \mu\text{mol}/\text{m}^2$ ). The silane cleavage (not reported) was apparently only 13%.

Fazio *et al.* [24] introduced the use of peroxyoctanoic acid in ether for the oxidation of a propylthiol-derivatized silica with the “absence of significant hydrolysis” of the original silane. They reported a bonding density of  $4.1\ \mu\text{mol}/\text{m}^2$  for attachment of the propylthiol-derivatized silica. Using optimized conditions of 6 h in peroxyoctanoic acid in diethyl ether at room temperature, the authors obtained a maximum exchange capacity of 0.34 mequiv./g for the final phase and also stated that a maximum conversion from thiol to sulfonic acid of 50% was achieved. To explain the limited conversion, the authors theorized that the reaction proceeded through a disulfide intermediate so that only thiols adjacent on the silica surface could react to form the sulfonic acid. Isolated thiols would not react.

Because Fazio *et al.* [24] reported minimum silane cleavage, their scheme was chosen for investigation. In addition, a scheme to improve the yield of the thiol-to-sulfonic acid conversion

was devised, assuming that the reaction proceeds through the disulfide intermediate. The revised scheme involves preparation of an intermediate disulfide phase prior to peroxyoctanoic acid oxidation. If indeed isolated thiols are present, they should be converted to the disulfide by the intermediate reaction, and become oxidized to sulfonic acid in the subsequent step. The original scheme of Fazio *et al.* and the revised disulfide intermediate scheme are depicted in Fig. 1.

#### Set 1: propylthiol attachment

Two sets of propylthiol silane attachments, disulfide couplings, and peroxyoctanoic acid oxidation experiments were conducted using two different base silicas: Waters Nova 5  $\mu\text{m}$  and Davisil. In the first set, a 6-g batch of propylthiol-derivatized Waters silica was prepared by reacting 3-mercaptopropyltrimethoxysilane with silica in toluene overnight under reflux. The reacted phase was washed with methanol ( $12\times$ ) and air dried. The final phase had a bonding density of  $1.87\ \mu\text{mol}/\text{m}^2$  (%C) or  $1.65\ \mu\text{mol}/\text{m}^2$  (%S). The %C calculation assumes that only one of the methoxy leaving groups has reacted and that the other two are still present on the attached ligand. If it assumed that all three methoxy leaving groups are reacted, %C analysis predicts a bonding density of  $3.20\ \mu\text{mol}/\text{m}^2$ ! Due to the ambiguity associated with the carbon

analysis, the bonding density associated with the percent sulfur analysis is believed to be more accurate. Sulfur analysis is used to track the course of the reaction.

#### Set 1: disulfide couplings

Next, two different 2-g portions of the Waters propylthiol silica were reacted in 20–30 ml of 35% diethyldisulfide in DMSO. The reagents were weighed in a dry box and the reactions were conducted under a dry nitrogen blanket. DMSO was used as the solvent because it is also known to oxidize thiols to disulfides [25,26], and should ensure the completeness of the reaction. The reaction conditions were 14 h at  $160^\circ\text{C}$  for the first portion and 22 h at  $70\text{--}96^\circ\text{C}$  (imprecise temperature control) for the second portion. The disulfide reaction was successful as evidenced by a correlated increase in both %C and %S analysis. The  $\Delta\%C$  and  $\Delta\%S$  can be used to calculate the amount of disulfide ligand produced if it is assumed that no silane cleavage occurred. This assumption is made for the benefit of calculation only, and as discussed later, is probably not true.  $\Delta\%C$  and  $\Delta\%S$  calculations gave similar results: *ca.*  $1.2\ \mu\text{mol}/\text{m}^2$  of disulfide was obtained for the higher temperature reaction (“high disulfide”) vs.  $0.6\ \mu\text{mol}/\text{m}^2$  for the lower temperature reaction (“low disulfide”). IR spectra were taken of the original thiol, and the high- and

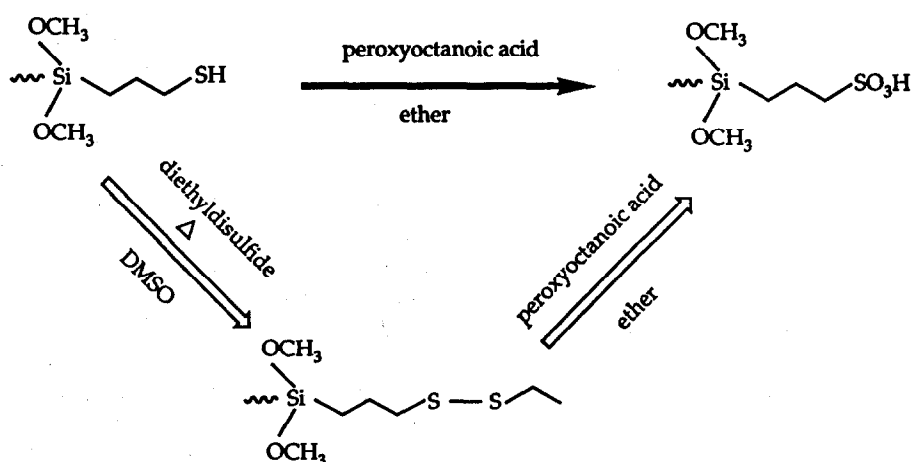


Fig. 1. Schemes to produce a sulfonic acid phase via direct oxidation of a thiol phase according to Fazio *et al.* [24] (solid arrows) or via oxidation of an intermediate disulfide phase (open arrows).

low-disulfide phases. Weak methyl and/or methylene signals could be observed for all three phases in the 3000–2850  $\text{cm}^{-1}$  range. The intensity of the 2938  $\text{cm}^{-1}$  band increased and the intensity of the 2857  $\text{cm}^{-1}$  band decreased in going from the thiol to low-disulfide to high-disulfide phase. The S–H band for the thiol phase was barely discernible at 2579  $\text{cm}^{-1}$ . A spot test was able to detect the thiol functional group for the thiol phase as reported at the end of the next section.

#### Set 1: peroxyoctanoic acid oxidations

The thiol and disulfide phases were subsequently oxidized by reacting 1 g of the phase in 50 ml of 0.4 M peroxyoctanoic acid in diethyl ether; the reaction was run for 6 h at room temperature (22°C). Because peroxyoctanoic acid is unstable, it must be prepared just before use. The procedure, previously used by Fazio *et al.* [24], is detailed by Parker *et al.* [27] and involves the stoichiometric reaction of hydrogen peroxide with octanoic acid in concentrated sulfuric acid to produce peroxyoctanoic acid. The freshly prepared peroxyoctanoic acid is extracted into diethyl ether, and the ether solution is washed several times with water to remove traces of sulfuric acid. A 150-ml volume of 0.4 M peroxyoctanoic acid in diethyl ether was prepared in this manner and then split into thirds for immediate use in this experiment. Three sulfonic acid phases were produced: oxidized thiol, oxidized “high disulfide” and oxidized “low disulfide”. The sulfonic acid phases were washed with methanol (5×), water (3×), methanol again (3×), and then characterized by elemental analysis (%C, %S) and acid–base titration.

In addition to calculating exchange capacities, the acid–base titration curves were used for qualitative phase characterization. The shape of the titration curve identifies the titrated species as a strong or weak acid. The ability to discriminate between strong and weak cation exchangers was demonstrated by titrating a commercial strong cation-exchange phase (Supelco SCX, a propylsulfonic acid phase, base silica 175  $\text{m}^2/\text{g}$ ) and a commercial weak cation-exchange phase

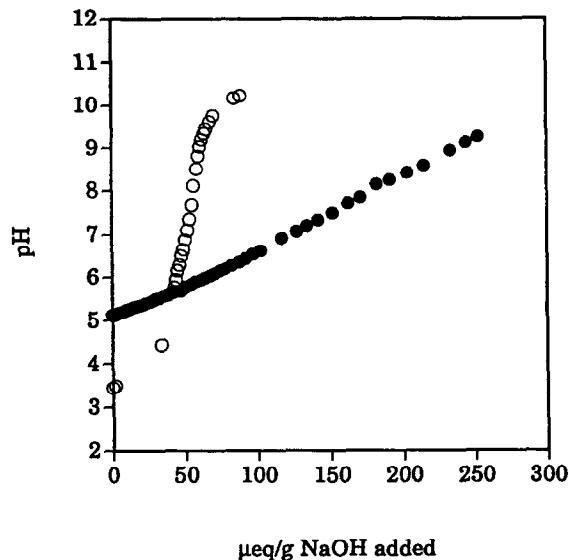


Fig. 2. Acid–base titration of commercial cation-exchange phases: Supelco SCX, a propylsulfonic acid phase (○) and Alltech RP4/Cation, a butanoic acid phase (●).

(Alltech RP4/Cation, a butanoic acid phase, base silica 350  $\text{m}^2/\text{g}$ ). The titration curves are shown in Fig. 2 as pH vs.  $\mu\text{equiv.}_{\text{NaOH}}/\text{g}_{\text{silica}}$  added. The titration curve for the sulfonic acid phase is a steep S-shaped curve; the titration curve for the carboxylic acid phase is characteristic of a weak acid. The difference between the shapes of the two titration curves is somewhat exaggerated in this plot because the exchange capacity of the carboxylic acid phase is four times higher than the sulfonic acid phase.

Titration curves for the three Waters sulfonic acid phases are given in Fig. 3, and confirm that strong acid phases were produced. Results show that the highest conversion to sulfonic acid was obtained by direct oxidation of the propylthiol phase (46  $\mu\text{equiv.}/\text{g}$ ), and that disulfide coupling does not increase the final yield. The exchange capacity of the sulfonic acid phase produced from the high-disulfide phase (43  $\mu\text{equiv.}/\text{g}$ , 160°C) was higher than the capacity of the sulfonic acid phase produced from the low-disulfide phase (29  $\mu\text{equiv.}/\text{g}$ , 70–96°C). Cleavage of the propylthiol ligand was 24% (%S) based on the direct thiol oxidation case. Silane cleavage could not be calculated for the

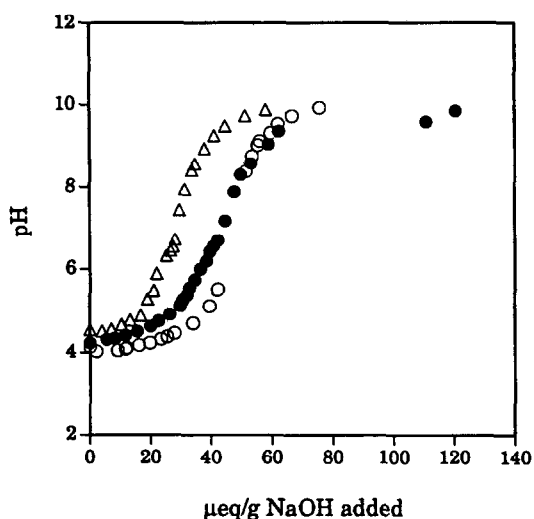


Fig. 3. Acid–base titration of laboratory-made sulfonic acid phases (Waters base silica): oxidized thiol (○), oxidized “high disulfide” (●) and oxidized “low disulfide” (△).

sulfonic acid phases produced from the disulfide phases, because the amount of residual disulfide was unknown.

A spot test was used to determine if unreacted thiol groups were present on the various phases. The test is based on the reaction of alcoholic ammoniacal sodium nitroprusside with thiols [28]; disulfides and sulfonic acids do not react. Four drops of the reagent were added to 30 mg of the phase to be tested in a test tube. A pinkish-purple color develops within 1 min if the test is positive. The propylthiol phase, disulfide phases, sulfonic acid phases and the underivatized Waters silica were all tested in this manner. Only the propylthiol phase gave a positive result.

#### Set 2

Because the amount of silane cleavage introduced by the disulfide coupling step was unknown, and the sulfonic acid phase produced from the high-disulfide phase had an exchange capacity close to the sulfonic acid phase produced by direct thiol oxidation, a second set of experiments was conducted to determine if a net increase in final sulfonic acid yield could be obtained from disulfide couplings conducted at intermediate temperatures. A higher surface

area silica (Davisil, 300 m<sup>2</sup>/g) was used to emphasize the difference in μequiv./g exchange capacities. Propylthiol attachment produced a phase with 1.63 (%C) or 1.69 (%S) μmol/m<sup>2</sup> bonding density consistent with the coverage achieved with the Waters silica. Two disulfide couplings were run at intermediate temperatures: 131 and 119°C, and produced disulfide phases with bonding densities for the disulfide ligand of 0.84 (131°C) and 0.66 (119°C) μmol/m<sup>2</sup> based on Δ%S; these disulfide bonding densities are intermediate between the bonding densities obtained for the Waters silica 160°C coupling (1.25 μmol/m<sup>2</sup>) and 70–96°C coupling (0.50 μmol/m<sup>2</sup>) as shown in Fig. 4. A good correlation between temperature of the reaction and disulfide “bonding density” is observed.

Peroxyoctanoic acid oxidations using 1.7 M peroxyoctanoic acid in diethyl ether were carried out for 6 h at room temperature. A more concentrated reagent was made due to the higher surface area of the silica. Once again, the maximum exchange capacity calculated from the

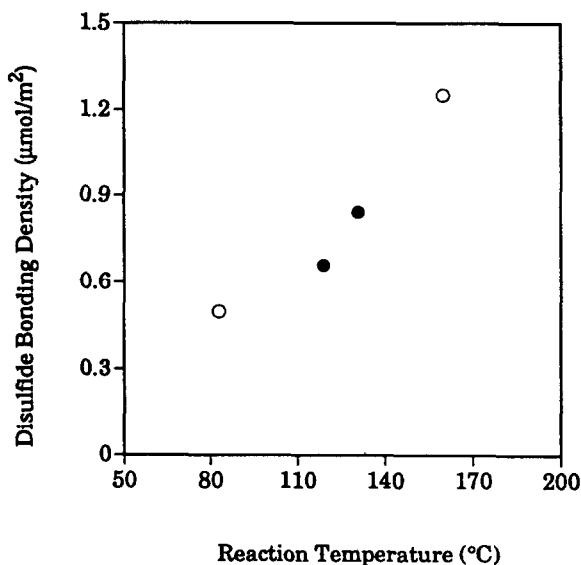


Fig. 4. The effect of reaction temperature on the disulfide coupling step using Waters (○) and Davisil (●) base silicas. The bonding density is calculated from the difference in %S of the phase before vs. after reaction and does not account for cleavage of the propylthiol ligands which may occur. The average temperature is used for the lower point of the Waters phase.

titration curves was obtained via direct oxidation of the propylthiol phase (283  $\mu\text{equiv./g}$ ), and the sulfonic acid phase produced from the high-disulfide phase (223  $\mu\text{equiv./g}$ , 131°C) had a higher capacity than that produced from the low-disulfide phase (212  $\mu\text{equiv./g}$ , 119°C). The difference was less pronounced because the temperature difference was smaller. Cleavage (%S) based on the direct thiol oxidation phase was 30%.

The exchange capacity of the phase produced in the second set was 0.94 vs. 0.39  $\mu\text{mol/m}^2$  in the first set. The efficiency of the peroxyoctanoic acid oxidation in the second set of reactions (56%) was more than twice as much vs. the first (24%) based on the percentage of the original propylthiol ligands that were converted to active sulfonic acid ligands for the direct thiol oxidations. The concentration of peroxyoctanoic acid was four times higher for the second set of reactions (1.7 M) vs. the first (0.41 M), although the actual molar excess was two times lower for the second set (76:1) vs. the first (150:1). This indicates that the concentration of peroxyoctanoic acid is likely a key factor in the efficiency of the oxidation reaction, because all other factors and results for the two sets of reactions are similar. This difference in oxidation efficiency is also observed for the disulfide coupled phases.

A commercial propylsulfonic acid phase, Supelco SCX, was characterized for comparison to the laboratory-made phases. Elemental analysis (%S) indicated that the propylsulfur-containing ligand is present at more than 3  $\mu\text{mol/m}^2$  (assuming 1 S atom per ligand), but the amount of active propylsulfonic acid ligand (exchange capacity) is only 0.3  $\mu\text{mol/m}^2$ . Therefore, only 10% of the propylsulfur ligand precursor was converted to sulfonic acid. The pH of the Supelco SCX silica dispersion prior to titration was ca. 3.9, which is slightly lower than the pH of the sulfonic acid phase dispersions produced here, so that the low capacity is not due to preneutralization by the manufacturer. Therefore, the results obtained in this research represent higher yields than at least one commercially available phase.

A spot test using pinacryptol yellow for the detection of sulfonates reagent [29] was evaluated. The test is based on the exchange of the dye reagent's counterion with the sulfonate, and the subsequent effect on the dye's fluorescent properties. Unfortunately, the reagent was available with a methanesulfonate counterion only, and therefore the anion exchange (methanesulfonate vs. propylsulfonate) did not change the fluorescent properties significantly enough for visual detection.

The results for the thiol and sulfonic acid phases are summarized in Table 2. Note that the bonding densities calculated from %S analysis correlate with the bonding densities calculated from %C analysis for both the propylthiol phases (part A) and the sulfonic acid phases produced via direct oxidation (part B). The %C calculation assumes that only one of the methoxy groups of the propylthiol silane ligand has reacted. This is a good assumption since the reactions were conducted under anhydrous conditions. The percentage of total ligand which is active can be calculated for the sulfonic acid phases (part B) from the exchange capacity ( $\mu\text{mol/m}^2$ ) and the bonding density (%S). The percent active ligand is 31% for the Waters sulfonic acid phase and 79% for the Davisil sulfonic acid phase, reiterating the higher conversion obtained in the second set of peroxyoctanoic acid oxidations. Although the conversion was significantly higher in the second set of reactions, the amount of silane cleavage (30%) was not significantly higher than in the first set (24%).

If it is assumed that there is no residual disulfide, the bonding densities calculated from both %S and %C analysis for the sulfonic acid phases produced via the disulfide intermediate (part C) indicate that the *total* amount of ligand is higher than the phases produced by direct oxidation (part B). If residual disulfide is present, then there could actually be less total ligand for these phases. In either case, the final amount of *active* ligand is lower for the sulfonic acid phases produced via the disulfide intermediate. Since it is expected that a disulfide is easier to oxidize than a thiol, it is likely that the lower net



Table 2  
Summary of propylthiol and sulfonic acid phases

Silica	Temperature disulfide coupling (°C)	Bonding density ( $\mu\text{mol}/\text{m}^2$ )		Exchange capacity		Active ligands %	Cleavage % <sup>c</sup>
		%C	%S	$\mu\text{mol}/\text{m}^2$	$\mu\text{equiv.}/\text{g}$		
<i>A. Propylthiol phases</i>							
Waters		1.87 <sup>a</sup>	1.65				
Davisil		1.63 <sup>a</sup>	1.69				
<i>B. Sulfonic acid phases via direct oxidation of thiol phases</i>							
Waters		1.02 <sup>b</sup>	1.25	0.39		31	24
Davisil		1.07 <sup>b</sup>	1.19	0.94		79	30
<i>C. Sulfonic acid phases via disulfide intermediate phases</i>							
Waters	70–96	1.21 <sup>b,d</sup>	1.50 <sup>d</sup>	0.24	29		
Waters	160	1.35 <sup>b,d</sup>	1.61 <sup>d</sup>	0.36	43		
Davisil	119	1.32 <sup>b,d</sup>	1.50 <sup>d</sup>	0.71	212		
Davisil	131	1.32 <sup>b,d</sup>	1.50 <sup>d</sup>	0.74	223		

<sup>a</sup> Calculated assuming 5 carbons per propylthiol ligand.

<sup>b</sup> Calculated assuming 5 carbons per propylsulfonic acid ligand.

<sup>c</sup> Based on sulfur analyses.

<sup>d</sup> Calculated assuming no residual disulfide is present.

yield is due to additional silane cleavage which occurred in the disulfide coupling step.

Fazio *et al.* [24] reported a maximum conversion of 50% for direct oxidation of a thiol phase to a sulfonic acid phase using peroxyoctanoic acid in diethyl ether. We obtained 24 or 56% conversion with the higher conversion corresponding to higher peroxyoctanoic acid concentration. The concentration of peroxyoctanoic acid should be pursued as a key factor in further attempts to optimize this reaction.

### 3.2. Carboxylic acid, carboxylate phases

There are a few reports of carboxylic acid phases in the literature. Asmus *et al.* [30] prepared a carboxymethylphenyl phase via a three-step reaction sequence: (1) attachment of a chloromethylphenyl ligand, (2) conversion of the chlorine group to a cyano group with  $\text{CN}^-$  and (3) oxidation of the cyano group with a mixture of concentrated sulfuric and acetic acids. The final phase had a capacity of 130  $\mu\text{equiv.}/\text{g}$  (0.33  $\mu\text{mol}/\text{m}^2$ ). Chang *et al.* [31] prepared a carbox-

ymethyl-derivatized silica by attachment of  $\gamma$ -glycoxypropylsilane followed by oxidation with a sodium metaperiodate, potassium carbonate, potassium permanganate reagent. Ion-exchange capacities for two different base silicas were reported in units of  $\text{mg}_{\text{hemoglobin}}/\text{ml}_{\text{derivatized silica}}$  and were 19 (70  $\text{m}^2/\text{g}$  silica) and 38 (130  $\text{m}^2/\text{g}$  silica). Caude and Rosset [32] prepared a polymeric carboxylate-derivatized silica by first attaching a vinyl silane and subsequently copolymerizing methacrylic acid with the vinyl silica. An exchange capacity of 2.2 mequiv./g (5.5  $\mu\text{mol}/\text{m}^2$ ) was reported. Kolla *et al.* prepared a series of polymeric carboxylate-derivatized based on 1:1 butadiene–maleic acid polymers [38]. The preformed butadiene–maleic acid polymers were physisorbed onto silica at several different film thicknesses, and subsequently crosslinked to the silica surface to provide covalent linkage. The resulting exchange capacities were a direct function of film thickness with reported values ranging from 1.1 to 3.9 mmol/g (2.9 to 10  $\mu\text{mol}/\text{m}^2$ ). Khurana *et al.* [33] used direct coupling of a commercially available carboxylic acid silane

(carboxypropyldimethylchlorosilane) to silica. The reported exchange capacity (acid–base titration) was 90  $\mu\text{equiv./g}$  ( $0.23 \mu\text{mol/m}^2$ ).

Thus, there appears to be no general way of preparing a carboxylic acid phase, and except for the polymeric phases, the bonding densities of active ion exchanger are low. One scheme that has not been reported is the attachment of an ester-containing silane followed by hydrolysis to the carboxylic acid or carboxylate. A search was conducted to determine a suitable hydrolysis method given that the pH stable range for bonded phases is approximately 2.5 to 7.5. Acids cause cleavage of the silane from the surface (Si–C bond cleavage) and bases dissolve the silica backbone (Si–O bond cleavage).

One hydrolysis technique that appeared promising is the hydrolysis of methyl esters using lithium halide salts in DMF [34]. DMF has been used as a solvent for silane–silica couplings. This scheme is depicted in Fig. 5A. When it became clear that significant silane cleavage (25–50%) did in fact occur with lithium halides in DMF, acidic hydrolysis was also pursued (Fig. 5B). The efficiency of hydrolysis under the acidic conditions tested was also low with significant silane cleavage (50%). Despite the low conversions obtained, both reactions were successful, and the results are presented for the researcher who wishes to continue in this area.

#### Ester phases

Two different ester silanes were used to prepare ester-derivatized silicas: (10-carbomethoxydecyl)dimethylchlorosilane ( $\text{C}_{11}$  ester) and 2-

(carbomethoxyethyl)methyldichlorosilane ( $\text{C}_3$  ester). Reactions were run overnight in refluxing dichloromethane. In most of the reactions, DMAP was added as a catalyst to increase the bonding density. After the reaction was completed, the derivatized silicas were washed three times each with dichloromethane, methanol, methanol–water (1:1), methanol again, and finally, diethyl ether. The silicas were then air dried overnight and stored in a desiccator. The  $\text{C}_{11}$  ester silane was coupled to Waters Nova 12- $\mu\text{m}$  silica both without and with DMAP catalyst to produce low- and high-bonding-density ester phases of 1.88 and  $3.21 \mu\text{mol/m}^2$  (%C), respectively. The  $\text{C}_3$  ester silane was coupled to both Waters Nova 5- $\mu\text{m}$  and Supelco silicas using DMAP catalyst to produce high-bonding-density phases of 3.08 and  $2.96 \mu\text{mol/m}^2$ , respectively. Results are tabulated in Table 3 (part A). High-bonding-density ester phases (*ca.*  $3 \mu\text{mol/m}^2$ ) were consistently produced when the DMAP catalyst was used.

The IR spectrum of the high-bonding-density  $\text{C}_{11}$  ester phase is given in Fig. 6 vs. the spectrum for the underivatized silica. The methylene and carbonyl bands for the ester phase are easily observed on top of the silica background. The carbonyl region comprises a major peak at  $1749 \text{ cm}^{-1}$  and much smaller peak at  $1720 \text{ cm}^{-1}$ . The peak at  $1749 \text{ cm}^{-1}$  corresponds to the normal carbonyl stretch observed for long-chain aliphatic esters. Note the disappearance of the SiOH band at  $3738 \text{ cm}^{-1}$  (isolated silanols) in going from the underivatized silica to the ester phase.

We expected the spectrum of the low-bonding-

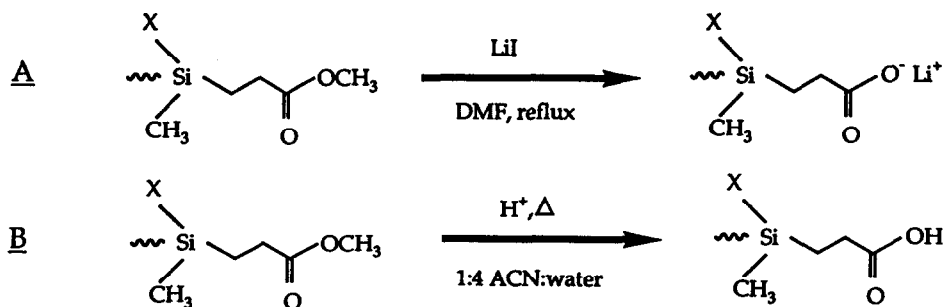


Fig. 5. Schemes to produce carboxylic acid phases based on the hydrolysis of an ester using lithium hydroxide in DMF (A) and aqueous acid (B). ACN = Acetonitrile.

Table 3  
Summary of ester and carboxylic acid phases

Silica	Ester chain length	DMAP catalyst	Bonding density ( $\mu\text{mol}/\text{m}^2$ )	Reaction time (min)	HCl (%)	Reaction temperature ( $^{\circ}\text{C}$ )	Exchange capacity		Cleavage (%)
							$\mu\text{mol}/\text{m}^2$	$\mu\text{equiv.}/\text{g}$	
<i>A. Ester phases</i>									
Waters Nova 12 $\mu\text{m}$	C <sub>11</sub>	No	1.88						
Waters Nova 12 $\mu\text{m}$	C <sub>11</sub>	Yes	3.21						
Waters Nova 5 $\mu\text{m}$	C <sub>3</sub>	Yes	3.08						
Supelco	C <sub>3</sub>	Yes	2.96						
<i>B. Carboxylic acid phases: lithium iodide/DMF hydrolysis time study</i>									
				2			0.29	34	
				19			0.32	38	
				271			0.26	31	
				328			0.16	19	
<i>C. Carboxylic acid phases: acidic hydrolysis acid level study</i>									
					0.1	92	0.20	34	49
					0.5	92	0.12	21	46
					1	83	0.24	41	41
					5	83	0.23	39	51

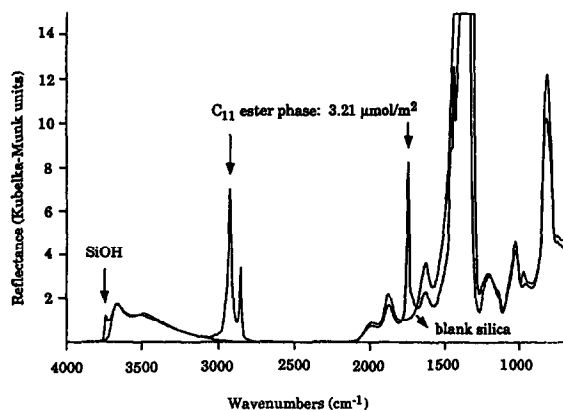


Fig. 6. Diffuse reflectance infrared spectrum of high-bonding-density  $C_{11}$  ester phase vs. the spectrum of the blank silica. Base silica is Waters Nova 12  $\mu\text{m}$ .

density  $C_{11}$  ester phase to resemble the high-bonding-density spectrum but with a lower intensity for the alkyl and carbonyl bands. We did, indeed, observe this in the alkyl region, but the carbonyl bands for the low-bonding-density phase showed a reversal in the relative intensity of the two carbonyl peaks. An enlargement of the carbonyl band region for the two ester phases is given in Fig. 7. The high bonding density phase has a large peak at  $1749\text{ cm}^{-1}$  and a much smaller peak at  $1720\text{ cm}^{-1}$ , whereas the same peaks in the low-bonding-density phase spectrum are closer in intensity with the  $1720$

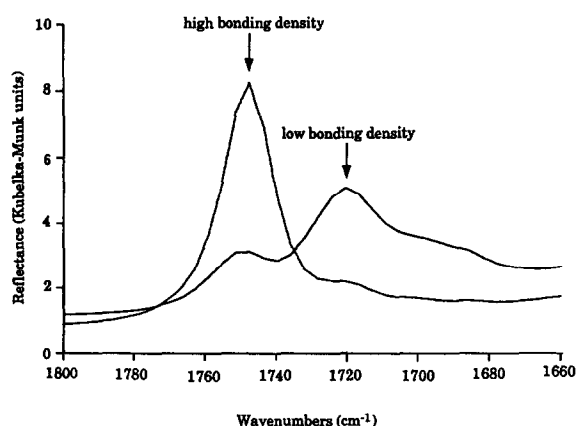


Fig. 7. Diffuse reflectance infrared spectra of high- ( $3.21\ \mu\text{mol}/\text{m}^2$ ) and low- ( $1.88\ \mu\text{mol}/\text{m}^2$ ) bonding-density  $C_{11}$  ester phases. Base silica is Waters Nova 12  $\mu\text{m}$ .

$\text{cm}^{-1}$  peak being larger. There are two possibilities to explain the peak at  $1720\text{ cm}^{-1}$ : (1) some hydrolysis of the ester has already occurred, and the peak corresponds to carboxylic acid; this possibility was eliminated based on titration with sodium hydroxide; and (2) hydrogen bonding between the carbonyl oxygen of the ester and the silica surface silanols lowers the carbonyl stretching frequency for a given population of the covalently bound ligands; this explanation is consistent with the observed increase in the  $1749\text{ cm}^{-1}$  peak in going from low to high bonding density. As the surface becomes more crowded, there is less possibility for the carbonyl moiety, which is at the opposite end of the molecule, to hydrogen bond with the silica surface. An IR spectrum was also taken of the Waters  $C_3$  ester phase. The carbonyl region comprised two equal intensity bands at  $1737$  and  $1716\text{ cm}^{-1}$  showing evidence of a dual ligand population.

Other researchers have seen evidence of ligand-to-surface hydrogen bonding and/or dual ligand populations (free vs. surface-hydrogen bonded) in the IR spectra of derivatized silicas. Suffolk and Gilpin [1] deconvoluted the cyano band of cyanoalkylsilanized silicas into high- and low-frequency components which were attributed to hydrogen bonded and free cyano ligands, respectively. Leyden *et al.* [4] attributed the simultaneous shifts of amide I (carbonyl) and amide II bands for acetoacetamide-functionalized silicas to hydrogen bonding of both the amide carbonyl and the amide NH with the silica surface.

#### Lithium halide hydrolysis

The initial lithium halide hydrolysis experiments were conducted with the  $C_{11}$  ester phases. A 1-g amount of the low-bonding-density ester phase was dispersed in 20 ml of DMF, and 0.50 g LiBr ( $27\times$  molar excess) were added (all done in dry box). The reaction was run for 3 h under nitrogen purge and reflux conditions. An IR spectrum of the reacted phase showed little to no change in the carbonyl group frequencies or intensities. %C analysis showed that 27% silane cleavage had occurred. The reaction was re-

peated with the high-bonding-density  $C_{11}$  ester phase, using a larger LiBr molar excess ( $71\times$ ), and a longer reaction time (22 h). The IR spectrum of the reacted phase resembled the IR spectrum of the low-bonding-density ester phase. %C analysis showed that 46% silane cleavage occurred. Our interpretation of these results is that no hydrolysis of the ester occurred in either case, and that the higher amount of cleavage in the second attempt was evident in the IR spectrum.

The original reference for the lithium halide hydrolysis [34] indicated that the rate of hydrolysis was higher for LiI (100% hydrolysis within 1.5 h) than LiBr (100% hydrolysis within 4 h). A final set of experiments was conducted to see if lithium iodide was more reactive. In addition, the reaction was monitored as a function of time because the amount of silane cleavage was observed to increase with time in the previous experiments. The ester phase used was the Waters  $C_3$  methyl ester, and LiI was added at a  $26\times$  excess. Samples of the reacted silica were removed at various time intervals after the reaction mixture began to reflux (total reaction time 5.5 h). The samples were washed with acetone ( $6\times$ ), water ( $6\times$ ), pH 3.0 HCl ( $6\times$ ), water ( $6\times$ ) and acetone ( $3\times$ ), then air dried and analyzed for exchange capacity. The data are tabulated in Table 3 (part B), and show that the exchange capacity reached its maximum ( $38\ \mu\text{equiv./g}$ ) within the first 20 min and then decreased with time, probably due to subsequent silane cleavage. Silane cleavage was 58% after the first 2 min of the reaction, and 67% after 201 min. The increasing cleavage of the silane from the surface was also observed as a continuing decrease in the intensity of the carbonyl bands in the IR spectra of the reacted phase at 2, 48, 141 and 211 min. There was only a slight change in the carbonyl group frequencies of the original ester vs. the hydrolyzed ester phases.

Titration curves for the maximum capacity reacted phase sample, the original ester phase, and the blank silica are given in Fig. 8. The blank silica had a capacity of  $8\ \mu\text{equiv./g}$  and the original ester had a capacity of  $21\ \mu\text{equiv./g}$  indicating that the ester phase has self-hydro-

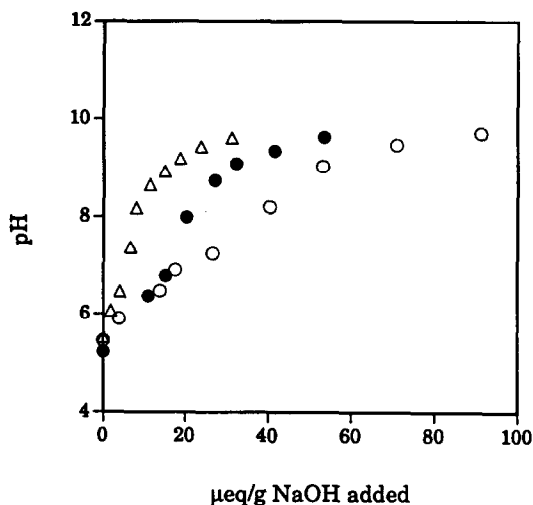


Fig. 8. Acid–base titration of propionic acid phase produced via lithium iodide hydrolysis of a  $C_3$  ester phase (○) vs. original  $C_3$  ester phase (●) and blank silica (△). Base silica is Waters Nova 5  $\mu\text{m}$ .

lyzed to a small extent, and show that although the capacity of the reacted phase is low, it is real.

#### Acidic hydrolysis

The initial acidic hydrolysis experiment was conducted by reacting 1 g of the high-bonding-density  $C_{11}$  ester phase in 60 ml of acetonitrile–water (1:1) at a pH of 4 (HCl). The reaction was run under reflux for 22 h. Silane cleavage was extremely low (0.18%) and an IR spectrum of the reacted phase showed no change from the original ester spectrum.

Since there was no evidence of reaction at pH 4, increasing acid levels were tested. The ester phase used was the Supelco  $C_3$  methyl ester. Hydrochloric acid levels of 0.1, 0.5, 1 and 5% were used with a constant reaction time of 22 h. For each of the runs, 1.5 g of the ester phase were dispersed in 20 ml of the acid in acetonitrile–water (1:4). (Acetonitrile is added to promote phase wetting. Less was needed here for the short-chain ester). The temperature for the 0.1 and 0.5% runs was  $83^\circ\text{C}$  and for the 1 and 5% runs  $92^\circ\text{C}$ . After washing, the final phases were titrated indicating low but real conversion (Fig. 9) and analyzed for %C. Exchange capacities of 21–41  $\mu\text{equiv./g}$  were obtained

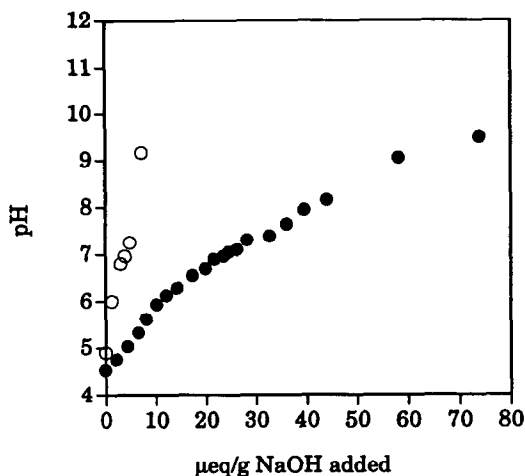


Fig. 9. Acid–base titration of propionic acid phase produced via acidic hydrolysis of a C<sub>3</sub> ester phase (●) vs. original C<sub>3</sub> ester phase (○).

(Table 3, part C) vs. a capacity of 6  $\mu\text{equiv./g}$  for the original ester. Despite the large range of acid levels tested (a 50:1 concentration range), silane cleavage varied over a narrow range of 41–51%. Capacities are low (21–41  $\mu\text{equiv./g}$ ), and the higher capacities were obtained with the higher acid levels, 1 and 5%.

The pH of the 0.1% HCl solution is theoretically 1.6. Based on the initial experiment, no reaction occurred at a pH of 4. Thus, it appears that once a threshold level of acid is reached (somewhere between pH 4 and 1.6), silane cleavage occurs to a significant extent but does not increase in proportion to the additional amount of acid added. Temperature may also be a factor but its effect was not intentionally studied here.

Low conversion to the carboxylate/carboxylic acid and significant ester silane cleavage were obtained for both lithium halide and acid hydrolysis schemes. The capacity of a commercial butanoic acid phase (Alltech RP4/Cation) was 200  $\mu\text{equiv./g}$  (0.57  $\mu\text{mol/m}^2$ ). Thus, the capacities obtained via lithium halide or acidic hydrolysis are 2–5 times less than a commercial phase.

It is likely that further optimization of the reaction conditions could improve the net yield for both hydrolysis reactions. The lithium halide

reactions were conducted under reflux conditions (153°C). Lower temperatures may provide similar conversion with less cleavage. The relative reactivities of lithium bromide and lithium iodide for ester hydrolysis and silane cleavage should also be investigated.

Silane cleavage from acidic hydrolysis varied from only 41 to 51% over a wide range of acid levels tested (0.1–5%), and there was no definite correlation between acid level and cleavage. Temperature may also be a factor but there are insufficient data to make a conclusion. Two avenues which may be promising to increase the net yield are higher acid levels (>5%) at lower temperatures (<80°C) to increase conversion, and lower acid levels under reflux conditions (100°C) to minimize silane cleavage. High temperature alone does not cause silane cleavage as evidenced by the pH 4 hydrolysis run for which there was less than 0.2% cleavage.

### 3.3. Quaternary ammonium phases

The synthesis of aliphatic quaternary ammonium-derivatized silica phases has not been reported although these phases are available commercially. A quaternary ammonium silane in which one of the nitrogen substituents is a C<sub>18</sub> alkyl chain is available from Huls for direct coupling to silica, but shorter-chain versions are not available.

A synthetic route that is frequently used to prepare aromatic quaternary ammonium derivatized silicas involves the direct reaction of a chloroalkyl-derivatized silica with a tertiary amine, or conversion of a chloroalkyl phase to an iodoalkyl phase followed by reaction with a tertiary amine. The aromatic moiety originates from either the chloroalkyl phase [35] or the tertiary amine [36,37]. In the cited references, reaction conditions were adjusted according to the volatility of the amine used. With benzyldimethylamine (boiling range 65–68°C), overnight reflux at 56 to 101°C was used. With TMA (boiling point –4°C), the reaction conditions were one week at 0°C.

The scheme presented here is the reaction between an iodoalkyl precursor phase and TMA

to produce an aliphatic quaternary ammonium phase. The conditions of the reaction are devised so as to speed up the reaction via heat while minimizing loss of the TMA reagent.

#### Iodoalkyl precursor phases

Iodoalkyl phases were prepared as precursor phases for quaternization. Commercial iodoalkylsilanes are available for direct coupling to silica, and 3-iodopropyltrimethoxysilane was coupled to Waters Resolve silica by reacting overnight in refluxing toluene. After derivatization, the phase was washed 15 times with methanol and then air dried. Elemental analysis (%C, %I) was conducted. The bonding density obtained was  $2.57 \mu\text{mol}/\text{m}^2$  (%C) or  $3.28 \mu\text{mol}/\text{m}^2$  (%I). It has been our experience that bonding densities based on %I are about 30% higher than those based on %C.

Due to the potential for cross-reactivity with the iodine moiety on the silane, conventional catalysts cannot be used to increase the bonding density obtained for iodoalkyl silane couplings. Therefore, an attempt to prepare a higher-bonding-density iodoalkyl phase based on the substitution of a chloroalkyl phase with sodium iodide was made as per Crowther *et al.* [37]. Crowther *et al.* used sodium iodide in methyl ethyl ketone under reflux conditions to convert chloropropyl-derivatized silica to the iodopropyl form.

A high-bonding-density chlorobutyl phase was made by coupling 4-chlorobutyltrimethylchlorosilane to Waters Nova 12- $\mu\text{m}$  silica with DMAP catalyst in dichloromethane (overnight, reflux). The resultant phase had a bonding density of 3.40 (%C) or 3.43 (%Cl)  $\mu\text{mol}/\text{m}^2$ . Next, the chlorobutyl phase was reacted with NaI (15 $\times$  excess) in methyl ethyl ketone. The reaction was carried out under a nitrogen purge

and reflux conditions for 17 h. The iodobutyl phase was washed as follows: acetone (3 $\times$ ), acetone–water (1:1) (10 $\times$ ), acetone (7 $\times$ ). The phase was air dried and analyzed for %C, %Cl and %I.

The %C was used to calculate the total bonding density after reaction ( $3.23 \mu\text{mol}/\text{m}^2$ ) indicating that minimal silane cleavage occurred (*ca.* 5%). Bonding densities based on %Cl and %I were used to calculate the relative amounts of the chlorobutyl and iodobutyl ligands present, and showed that the sum of chlorobutyl and iodobutyl ligands ( $2.44 \mu\text{mol}/\text{m}^2$ ) was lower than the total bonding density ( $3.23 \mu\text{mol}/\text{m}^2$ ). An explanation for this is that some amount of the haloalkyl ligand was hydrolyzed to the alcohol. The final iodobutyl bonding density (*ca.*  $2 \mu\text{mol}/\text{m}^2$ ) was lower than that obtained with direct iodopropyl silane attachment ( $2.6 \mu\text{mol}/\text{m}^2$ ).

#### Quaternization reactions

In the first attempt, a reaction temperature of 15–20°C was maintained by immersing the reaction flask in a circulating water bath, and the reaction flask was capped. A 1-g amount of the iodobutyl phase was dispersed in 10 ml ethanol, and 2 ml of 25% TMA in methanol were added. The reaction was stirred for 24 h, after which another 1-ml aliquot of the TMA reagent was added. The reaction continued for a second 24 h. The phase was washed and elemental analysis was performed. No nitrogen was found indicating that no detectable reaction occurred. Silane cleavage (%C) was 24%.

In the second attempt (Fig. 10), the reaction flask itself was gently heated (34°C) and a condenser containing circulating ethylene glycol–water (1:1) cooled to –7°C was attached. A

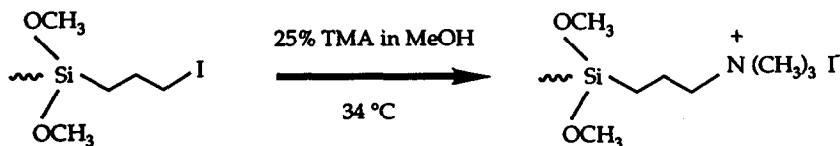


Fig. 10. Scheme to produce a C<sub>3</sub> quaternary ammonium phase based on the reaction of an iodopropyl phase with TMA using heat. Base silica is Waters Resolve.

Table 4  
Summary of quaternary ammonium phases

Mode of preparation	Silica	Bonding density ( $\mu\text{mol}/\text{m}^2$ )		Exchange capacity	
		%C	%N	$\mu\text{mol}/\text{m}^2$	$\mu\text{equiv.}/\text{g}$
Commercial silane	Waters Nova 12 $\mu\text{m}$	1.68	1.84	0.69	79
Quaternization of iodopropyl	Waters Resolve	1.86	0.92	0.52	91

2.6-g amount of the iodopropyl phase was dispersed in 25 ml of 25% TMA in methanol. The reaction was run for 22 h. Elemental analysis showed that quaternization had occurred (nitrogen found). The amount of nitrogen-containing ligand was  $0.92 \mu\text{mol}/\text{m}^2$  (based on %N), and the silane cleavage was 28% (based on %C). The exchange capacity was  $0.52 \mu\text{mol}/\text{m}^2$  ( $91 \mu\text{equiv.}/\text{g}$ ).

For comparison, a quaternary ammonium phase was prepared by direct coupling of the commercially available  $\text{C}_{18}$  quaternary ammonium silane (*n*-octadecyldimethyl[3-(trimethylsilyl)propyl]ammonium chloride) using Waters Nova 12- $\mu\text{m}$  silica. The reaction was conducted overnight in refluxing toluene. A bonding density of  $1.68 \mu\text{mol}/\text{m}^2$  (%C) or  $1.84 \mu\text{mol}/\text{m}^2$  (%N) was obtained. The exchange capacity was  $0.69 \mu\text{mol}/\text{m}^2$ .

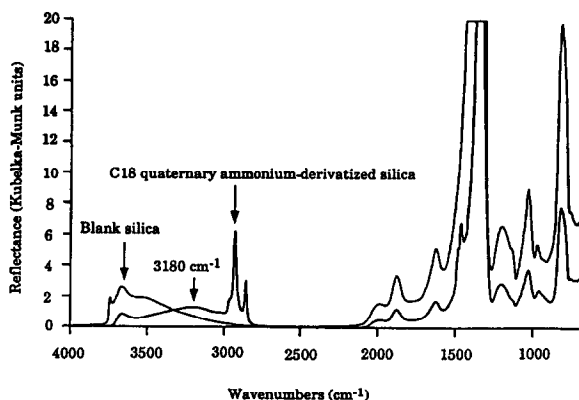


Fig. 11. Diffuse reflectance infrared spectrum of  $\text{C}_{18}$  quaternary ammonium phase produced via reaction of a commercial silane with Waters Nova 12- $\mu\text{m}$  silica.

An IR spectrum of the  $\text{C}_{18}$  quaternary ammonium phase was taken, and is shown in Fig. 11 vs. the underivatized silica spectrum. The methylene peaks at  $2930$  and  $2860 \text{ cm}^{-1}$  are apparent, but there is also a broad band with a peak frequency of  $3180 \text{ cm}^{-1}$ . This corresponds to an N–H stretch for an ammonium salt, and indicates that the amine is probably not 100% quaternized.

Results for the quaternary ammonium phases are summarized in Table 4. As expected, the %C and %N analyses predict a similar bonding density for the phase produced from coupling of the commercial silane. However, the bonding density calculated from %N is about 50% of the bonding density calculated from %C for the phase produced via the secondary quaternization reaction, which represents a rough estimate of the quaternization efficiency. The amount of active exchanger is less still, about 28% of the total and 57% of the nitrogen-containing ligands, respectively.

Further optimization of the reaction temperature, time and TMA concentration should be investigated for improving the quaternization efficiency. Also, the use of other tertiary alkyl amines which are less volatile than TMA would allow higher reaction temperatures and may give higher yields.

#### 4. Conclusions

The aliphatic ion exchangers produced have active exchange capacities of  $0.2$ – $0.9 \mu\text{mol}/\text{m}^2$ . Given that chromatographic silica is readily



available with surface areas up to 550 m<sup>2</sup>/g, the synthetic schemes presented can be used to produce phases with active capacities of 100–500  $\mu$ equiv./g. The suggested steps for further optimization are likely to provide even higher-capacity phases.

Characterization of derivatized silicas continues to represent a challenge to the analytical chemist. Functional group analysis is a key area. The best results are obtained when a combination of complimentary techniques is applied. IR analysis is most useful when the functional group absorbance does not overlap with the silica absorbance background, and when the bonding density of ligands and surface area of the base silica are sufficiently high. Spot tests can be used to supplement IR analysis, and as demonstrated here, can be more sensitive in certain cases.

## 5. Acknowledgements

The authors are grateful for support of this work by The National Forensic Chemistry Center of the FDA and NIEHS-04908. Special thanks to Sritana Yasui for obtaining all the IR spectra presented. Thanks also to Waters, Davisil, Supelco and Jones for donation of the silicas.

## 6. References

- [1] B.R. Suffolk and R.K. Gilpin, *Anal. Chim. Acta*, 181 (1986) 259.
- [2] B.R. Suffolk and R.K. Gilpin, *Anal. Chem.*, 57 (1985) 596.
- [3] L. C. Sander, J.B. Callis and L.R. Field, *Anal. Chem.*, 55 (1983) 1068.
- [4] D.E. Leyden, D.S. Kendall, L.W. Burggraf, F.J. Pern and N. DeBello, *Anal. Chem.*, 54 (1982) 101.
- [5] N. Watanabe, *Chem. Lett.*, (1981) 1373.
- [6] G.L. Berendsen and L. de Galan, *J. Liq. Chromatogr.*, 1 (1978) 561.
- [7] E. Bayer, K. Albert, J. Reiners, M. Nieder and D. Muller, *J. Chromatogr.*, 264 (1983) 197.
- [8] D.E. Leyden, D.S. Kendall and T.G. Waddell, *Anal. Chim. Acta*, 126 (1981) 207.
- [9] G.E. Maciel, D.W. Sindorf and V.J. Bartuska, *J. Chromatogr.*, 205 (1981) 438.
- [10] M.P. Fuller and P.R. Griffiths, *Anal. Chem.*, 50 (1978) 1906.
- [11] R.S.S. Murthy and D.E. Leyden, *Anal. Chem.*, 58 (1986) 1228.
- [12] P. Shah, L.B. Rogers and J.C. Fetzer, *J. Chromatogr.*, 388 (1987) 411.
- [13] R.C. Ziegler and G.E. Maciel, *J. Am. Chem. Soc.*, 113 (1991) 6349.
- [14] M. Gangoda, R.K. Gilpin and B.M. Fung, *J. Magn. Reson.*, 74 (1987) 134.
- [15] M. Verzele, P. Mussche and P. Sandra, *J. Chromatogr.*, 190 (1980) 331.
- [16] J.B. Crowther, S.D. Fazio, R. Schiksnis, S. Marcus and R.A. Hartwick, *J. Chromatogr.*, 289 (1984) 367.
- [17] S.D. Fazio, S.A. Tomellini, H. Shih-Hsien, J.B. Crowther, T.V. Raglione, T.R. Floyd and R.A. Hartwick, *Anal. Chem.*, 57 (1985) 1559.
- [18] H. Genieser, D. Gabel and B. Jastorff, *J. Chromatogr.*, 269 (1983) 127.
- [19] H. Genieser, D. Gabel and B. Jastorff, *J. Chromatogr.*, 244 (1982) 368.
- [20] J. Erard and E.sz. Kováts, *Anal. Chem.*, 54 (1982) 193.
- [21] L.M. Warth, R.S. Cooper and J.S. Fritz, *J. Chromatogr.*, 479 (1989) 401.
- [22] N. Weigand, I. Sebastian and I. Halász, *J. Chromatogr.*, 102 (1974) 325.
- [23] B.B. Wheals, *J. Chromatogr.*, 177 (1979) 263.
- [24] S.D. Fazio, J.B. Crowther and R.A. Hartwick, *Chromatographia*, 18 (1984) 216.
- [25] T.J. Wallace, *J. Am. Chem. Soc.*, 86 (1964) 2018.
- [26] C.N. Yiannios and J.V. Karabinos, *J. Org. Chem.*, 28 (1963) 3246.
- [27] W.E. Parker, C. Ricciuti, C.L. Ogg and D. Swern, *J. Am. Chem. Soc.*, 77 (1955) 4037.
- [28] G. Toennies and J.L. Kolb, *Anal. Chem.*, 23 (1951) 823.
- [29] H. Jork, W. Funk, W. Fischer and H. Wimmer, *Thin Layer Chromatography Reagents and Detection Methods*, Vol. 1a, VCH, New York, 1990.
- [30] P.A. Asmus, C. Low and M. Novotny, *J. Chromatogr.*, 123 (1976) 109.
- [31] S.H. Chang, K.M. Gooding and F.E. Regnier, *J. Chromatogr.*, 120 (1976) 321.
- [32] M. Caude and R. Rosset, *J. Chromatogr. Sci.*, 15 (1977) 405.
- [33] A.L. Khurana, E.T. Butts and C. Ho, *J. Liq. Chromatogr.*, 11 (1988) 1615.
- [34] P.D.G. Dean, *J. Chem. Soc.*, (1965) 6655.
- [35] P.L. Asmus, C. Low and M. Novotny, *J. Chromatogr.*, 119 (1976) 25.
- [36] G.B. Cox, C.R. Loscombe, M.J. Slucutt, K. Sugden and J.A. Upfield, *J. Chromatogr.*, 117 (1976) 269.
- [37] J.B. Crowther, S.D. Fazio and R.A. Hartwick, *J. Chromatogr.*, 282 (1983) 619.
- [38] P. Kolla, J. Kohler and G. Schomburg, *Chromatographia*, 23 (1987) 465.